

## Corrosion Inhibition Performance on Tubing Steel in Oil Wells Based on Schiff Base Surfactants

Yisheng Hu<sup>1\*</sup>, Yu Peng<sup>1</sup>, Weiyi Zhang<sup>2</sup>, Mingshan Song<sup>3</sup>

<sup>1</sup> State Key Laboratory of Oil and Gas Reservoir Geology and Exploitation, Southwest Petroleum University, Chengdu, 610500, China

<sup>2</sup> Drilling Fluid Technology Service Company, CNPC ChuanQing Drilling Engineering Company, Chengdu, 610056, China

<sup>3</sup> Petroleum Engineering Technology Institute, Southwest Petroleum Branch Company, SINOPEC, Deyang, 618000, China

\*E-mail: [huyisheng008@yahoo.com](mailto:huyisheng008@yahoo.com)

Received: 2 February 2017 / Accepted: 18 March 2017 / Published: 12 April 2017

---

The corrosion inhibition of mild steel at 25 °C in 1 M HCl with benzylidene-pyridine-2-yl-amine, (4-benzylidene)-pyridine-2-yl-amine, and (4-chloro-benzylidene)-pyridine-2-yl-amine were investigated in this study. Electrochemical and weight loss characterizations were employed to test the corrosion inhibition properties. The polarization curve indicates that the compounds used in this study are mixed type inhibitors. Moreover, the results suggest that the inhibition efficiency gradually increases with an increase in inhibitor concentration. Obvious differences in inhibition efficiencies were obtained by changing the functional group on the benzene ring. The corrosion behavior in the presence of inhibitors ( $10^{-2}$  M) was also investigated at various temperatures ranging from 25 to 43 °C. In addition, adsorption isotherms were calculated, using the Langmuir equation. Thermodynamic parameters and the associated activation energy of corrosion were determined. All results reveal that as currently used, Schiff base compounds show excellent corrosion inhibition properties.

---

**Keywords:** Schiff base surfactant; Corrosion; Deep oil well; Tubing steel; Surface tension

### 1. INTRODUCTION

Material loss on a metallic surface is a common problem caused by corrosion in saline media. Corrosion of oil wells is one of the most serious problems, particularly in the petroleum industry, because a large amount of formation water is extracted as a by-product of the oil-producing process. Unlike other waste water, numerous organic and inorganic compounds such as CO<sub>2</sub> and H<sub>2</sub>S are

dissolved in formation water. Therefore, formation water is considered one of the most corrosive liquids in the petroleum industry [1-3].

To protect oil wells from corrosion caused by formation water, development of corrosion inhibitors becomes very important for the petroleum industry. A large number of corrosion inhibition methods have already been developed. For example, organic substances show good corrosion inhibition properties [4-6]. Organic substances containing electro-negative functional groups, for instance hydroxyl groups, can be adsorbed onto the target surface. This effectively prevents the material from directly interacting with corrosive compounds such as water and CO<sub>2</sub> and results in a lower corrosion rate, thereby extending the working life of the target material. Nonionic surfactants have been well investigated as corrosion inhibitors for metals or alloys [7-14]. These nonionic surfactants can effectively decrease the concentration of micelle, and therefore contribute to higher corrosion inhibition. A series of Schiff base nonionic surfactants was developed by Migahed et al. [10]. EIS results showed that the concentration of those Schiff base nonionic surfactants can greatly improve the adsorption properties of surfactants on target materials. The inhibition performance of Tween-20, another Schiff base nonionic surfactant, on cold rolled steel was investigated by Li et al. [15]. The results suggested that the inhibition efficiency of Tween-20 gradually improved at higher concentrations. In addition, organic substances with heterocyclic compounds can be employed as cationic surfactants for corrosion inhibition, because oxygen, sulfur and nitrogen atoms can serve as anchor sites that contribute to the formation of an inhibition layer on the surface of target materials [16-19]. Therefore, Schiff base compounds can possess good corrosion inhibition properties, due to the presence of the —C=N group. A number of corrosion inhibitors with the —C=N group have been developed, representing a promising way to improve the performance of corrosion inhibition. More recently, a handful of Schiff base compounds were found to be very effective for the corrosion inhibition of aluminum, copper, zinc and mild steel in acid media [20-25].

In this study, a series of experiments, including chemical and electrochemical characterizations, was conducted to evaluate the corrosion inhibition of benzylidene-pyridine-2-yl-amine on mild steel at 25 °C in 1 M HCl. In addition, the substitution effect of a methyl group and chloride was investigated.

## 2. EXPERIMENTS

The Schiff bases used in this study were obtained by a condensation reaction. Generally, aldehydes (including benzaldehyde, 4-chloro benzaldehyde, 4-methyl benzaldehyde) and 2-aminopyridine were condensed in ethanol. The resulting products were recrystallized from ethanol. The resulting final inhibitors were (4-benzylidene)-pyridine-2-yl-amine, (4-chloro-benzylidene)-pyridine-2-yl-amine, and benzylidene-pyridine-2-yl-amine. A strong solution of HCl (37%, E. Merck) was used. A series of inhibitors (0.2 to 10 mM) was prepared using 1 M HCl. Double distilled water was employed for preparing all solutions.

X-65 tubing steel, a common material used in oil wells, was used for this study. The chemical analysis of X-65 tubing steel is listed in Table 1. The X-65 tubing steel was sliced into cuboids with

regular edges for weight loss analysis. For electrochemical and polarization investigation, a small piece of X-65 was used as an electrode after polishing. The surface area of the electrode was 1 cm<sup>2</sup>.

**Table 1.** Chemical analysis of X-65 tubing steel.

Element	C	Mn	Si	P	S	Ni	Cr	Mo	V	Cu	Al
Content (w/w)	0.07	1.47	0.37	0.02	0.07	0.03	0.02	0.01	0.006	0.05	0.06

A three-electrode cell, consisting of a mild steel working electrode (WE), a platinum counter electrode (CE), and a saturated calomel electrode (SCE) as a reference electrode, was used for measurements. All experiments were performed in atmospheric conditions without stirring.

A potentiostat–galvanostat (AUTOLAB) was employed for the polarization curve measurements. The data was then processed by GPES software in a Pentium IV computer. The scan range of potential was from –800 to –250 mV with a scan rate of 1 mV/s. Impedance was investigated using a computer-controlled potentiostat (AUTOLAB) under open circuit potential ( $E_{ocp}$ ) conditions, and the results were analyzed by FRA software. The frequency range of alternating current was adjusted from  $3 \times 10^{-2}$  to  $10^5$  Hz. The excitation signal was a 1 mV sine wave.

For investigating weight loss, the tubing steel was first sliced into small specimens (5 cm × 2 cm × 0.4 cm). The tubing steel specimens were then immersed for different time periods in an oil wastewater bath (chemical composition: Na<sup>+</sup>: 64 ppm; K<sup>+</sup>: 77 ppm; Ca<sup>2+</sup>: 4522 ppm; Mg<sup>2+</sup>: 997 ppm; Ba<sup>2+</sup>: 4.7 ppm; Sr<sup>2+</sup>: 89 ppm; Cl<sup>-</sup>: 107 ppm; SO<sub>4</sub><sup>2-</sup>: 196 ppm; HCO<sub>3</sub><sup>-</sup>: 288 ppm) with surfactant inhibitors, and the results were recorded. A control experiment was carried out under the same condition but without adding inhibitors. Distilled water was used to wash the corrosion products off the tubing steel surface. Then, the corrosion products and weight loss of the tubing steel were recorded and compared with those from previous experiments.

### 3. RESULTS AND DISCUSSION

The Nyquist plots of tubing steel measured at 25 °C in HCl solution (1 M) with and without additives [i.e., (4-benzylidene)-pyridine-2-yl-amine, (4-chloro-benzylidene)-pyridine-2-yl-amine, and benzylidene-pyridine-2-yl-amine] are shown in Fig. 1A-D. Concentration of additives were adjusted from  $2 \times 10^{-4}$  to  $1 \times 10^{-2}$  M. It is known that Nyquist plots are part of a semicircle. According to Haruyama and Tsuru [26], the difference in impedance between lower and higher frequencies can be utilized to calculate the charge transfer resistance values ( $R_t$ ). The frequency at which the imaginary component of the impedance is maximum ( $-Z_{i_{max}}$ ) was found, and the double-layer capacitance ( $C_{dl}$ ) was also calculated.

Using electrochemical impedance spectroscopy, the inhibition efficiency could be calculated using the resistance of charge transfer equation below:

$$\eta_z(\%) = \frac{R_{t(inh)} - R_t}{R_t(inh)} \times 100$$

where the values of the charge-transfer resistance towards mild steel in 1 M HCl in the absence of an inhibitor is represented by  $R_t$ , while in the presence of inhibitor, it is represented by  $R_{t(inh)}$ . The values of  $R_t$  increased with an increase in inhibitor concentration, although the values of  $C_{dl}$  tended to decline, because the inhibitor is adsorbed on the metal surface. The inhibition efficiency was found to increase with an increase in inhibitor concentration.

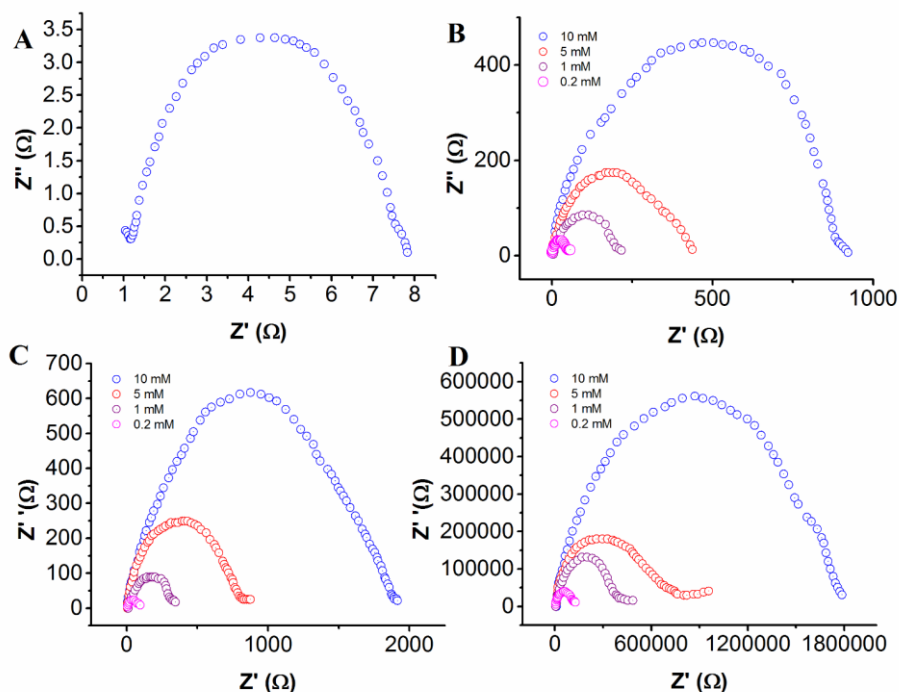


**Figure 1.** Nyquist plots of mild steel (A), benzylidene-pyridine-2-yl-amine (B), (4-benzylidene)-pyridine-2-yl-amine (C) and (4-chloro-benzylidene)-pyridine-2-yl-amine (D) in 1 M HCl at 25 °C.

**Table 2.** Impedance parameters and corresponding inhibition efficiency for corrosion of mild steel.

Inhibitor	$C_{inh}$ (M)	$R_t$ ( $\Omega$ cm <sup>2</sup> )	$C_{dl}$ ( $\mu$ F)	Inhibitor Efficiency ( $\eta$ z%)
Blank	–	7	355	–
benzylidene-pyridine-2-yl-amine	0.2	55	140	61.05
	1	51	71	88.62
	5	366	16	96.36
	10	1124	12	98.75
(4-benzylidene)-pyridine-2-yl-amine	0.2	17	151	54.28
	1	61	45	92.68
	5	499	13	95.41
	10	1322	7	98.63
(4-chloro-benzylidene)-pyridine-2-yl-amine	0.2	15	151	66.36
	1	63	71	97.21
	5	388	27	97.78
	10	1813	5	99.68

This indicates that the inhibitor molecules might be chemically adsorbed onto the steel surface, thereby covering some of the sites on the electrode surface. These adsorbed monomolecular layers are likely formed through the creation of a complex containing iron ions on the steel surface. In particular, these layers could protect the steel surface from being attacked by chloride ions. The results show that no interaction exists between the molecules that were adsorbed on the metal surface. The efficiencies of inhibition were ordered as follows: benzylidene-pyridine-2-yl-amine < (4-benzylidene)-pyridine-2-yl-amine < (4-chloro-benzylidene)-pyridine-2-yl-amine. The inhibition efficiency of the second and third compound in this list increases because of the substitution of the benzene ring with a methyl group and chloride ion, respectively, compared to the unsubstituted first compound in the list. For the Schiff bases, the  $-C=N$  group can form a strong  $\pi$  bond with the atoms in the benzene ring. Hence, the unoccupied orbitals of iron can accept the  $\pi$  electron of the Schiff bases. In fact, the  $\pi^*$  orbital can also accept d orbital electrons of iron to generate feed-back bonds resulting in the production of more than one chemical adsorption center. Moreover, the electron density of the nitrogen atom contained in the  $-C=N$  group increases when the Schiff base contains electron-donating groups such as (Cl,  $CH_3$ ), thereby inducing high inhibition efficiency. In addition, the electrostatic interaction with the negative-charged surface can also induce adsorption, such as the interaction between the positive-charged inhibitor and a particular adsorbed iron anion.

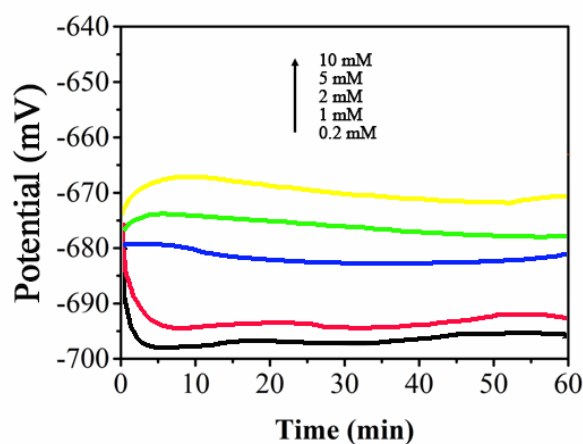


**Figure 2.** Plots of potential towards time for the tubed steel in the formation water of oil wells with (4-chloro-benzylidene)-pyridine-2-yl-amine of various concentrations.

The open circuit potential of the tubing steel electrode, which was exposed to formation water and synthesized Schiff base inhibitors for various periods, was also studied. It is clear from Figure 2 that a smaller (more negative) potential reading of the tubing steel electrode's open circuit was obtained when first immersed in the formation water. This is in keeping with other reports. However, the protective film generated on the electrode surface by the inhibitor primarily induces such behavior. In such cases, the open-circuit potential could shift slightly towards positive values.

Figure 3A-C illustrates both cathodic and anodic polarization curves of mild steel in 1 M HCl in the presence and absence of inhibitors of varying concentrations. The curves of cathodic current to potential result in parallel Tafel lines. This suggests that the reaction of hydrogen is activation-controlled. Therefore, the mechanism of this process cannot be modified by adding the Schiff bases used in this study [27]. In the case of corrosion potential, a larger negative shift occurs when adding a

Schiff base, in particular for high concentrations. For the curves of anodic current potential, the corrosion current increases dramatically when the concentration of inhibitors is high, especially for the substituted (4-chloro-benzylidene)-pyridine-2-yl-amine.

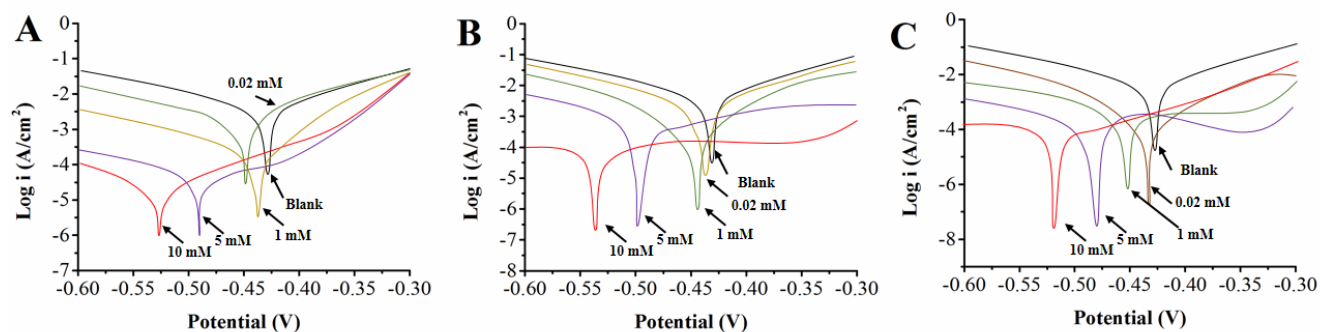


**Figure 3.** Polarization curves of the mild steel in hydrochloric acid (1 M) in the presence of (A) benzylidene-pyridine-2-yl-amine, (B) (4-benzylidene)-pyridine-2-yl-amine and (C) (4-chloro-benzylidene)-pyridine-2-yl-amine with various concentrations.

**Table 3.** Electrochemical polarization parameters for the mild steel in hydrochloric acid (1 M) containing different concentrations of benzylidene-pyridine-2-yl-amine, (4-benzylidene)-pyridine-2-yl-amine and (4-chloro-benzylidene)-pyridine-2-yl-amine.

Inhibitor	Concentration (M)	$E_{\text{corr}}$ (mV)	$I_{\text{corr}}$ ( $\text{mA}/\text{cm}^2$ )	$b_a$ (mV/dec)	$b_c$ (mV/dec)	Inhibition efficiency
Blank	-	-435	3.36	98	107	-
Benzylidene-pyridine-2-yl-amine	0.02	-441	2.20	96	105	34.67
	1	-488	0.155	55	89	95.39
	5	-502	0.307	107	121	98.95
	10	-535	0.352	109	129	99.08
(4-benzylidene)-pyridine-2-yl-amine	0.02	-451	1.56	88	110	53.68
	1	-496	0.106	76	111	96.82
	5	-501	0.364	96	127	98.91
	10	-544	0.216	104	135	99.35
(4-chloro-benzylidene)-pyridine-2-yl-amine	0.02	-465	1.11	77	97	67.04
	1	-488	0.135	48	88	95.99
	5	-511	0.0227	96	116	99.39
	10	-536	0.012	110	130	99.64

Such performance of Schiff bases is likely caused by the dissolution of the steel surface, resulting in the desorption of the Schiff base inhibitor that was previously absorbed on the surface of

the electrode. Both the anodic and cathodic reactions are influenced by adding the Schiff bases. Therefore, such compounds are recognized as mixed type inhibitors (anodic/cathodic). Moreover, the inhibitor efficiency obtained from the polarization measurements can be calculated using the following equation [28]:

$$\eta_p (\%) = \frac{I_{corr} - I_{corr(inh)}}{I_{corr}} \times 100$$

where the corrosion with and without inhibitors is represented by  $I_{corr(inh)}$  and  $I_{corr}$ , respectively. According to the results, the efficiency of inhibition in the presence of all the inhibitors studied improved with an increase in inhibitor concentration. Table 3 shows the polarization parameters in the presence and absence of various concentrations of Schiff bases and the corresponding inhibition efficiency.

Table 4 illustrates the weight loss measurement data of mild steel in hydrochloric acid (1 M) with and without inhibitors of varying concentrations. Inhibition efficiencies ( $\eta_w\%$ ) can be calculated using the following equation [29]:

$$\eta_w (\%) = \frac{W_{corr} - W_{corr(inh)}}{W_{corr}} \times 100$$

where the weight loss of mild steel with and without inhibitors is denoted as  $W_{corr(inh)}$  and  $W_{corr}$ , respectively. The results show that the inhibition efficiencies of all Schiff bases increase with an increase in inhibitor concentration. Moreover, the weight loss measurement data are in accordance with the results obtained through linear polarization and EIS measurements.

**Table 4.** The parameter of the mild steel corrosion at 25 °C in hydrochloric acid (1 M) with and without schiff bases of various concentrations obtained from weight loss characterizations.

Inhibitor	Concentration (mM)	Corrosion rate (mg/cm <sup>2</sup> ·h)	Surface coverage ( $\theta$ )	Inhibition efficiency ( $\eta_w$ )
Blank	–	5.521	–	–
benzylidene-pyridine-2-yl-amine	10	0.053	0.98	99.2
	5	0.092	0.967	98.8
	1	0.521	0.883	90.6
	0.2	2.55	0.567	57.5
(4-benzylidene)-pyridine-2-yl-amine	10	0.037	0.989	99.5
	5	0.081	0.982	98.3
	1	0.374	0.936	91.5
	0.2	2.68	0.517	56.6
(4-chloro-benzylidene)-pyridine-2-yl-amine	10	0.021	0.993	99.3
	5	0.081	0.988	98.4
	1	0.307	0.943	93.2
	0.2	1.689	0.692	65.3

A buffering layer was formed between the interface of the tubing steel surface and the oil well's formation water. This was confirmed through electrochemical measurement. Energy dispersive analysis (EDX) was carried out to analyze the composition of the buffering layer. The thickness of the buffering layer was evaluated with an Fe signal. The spectrum for polished tubing steel sample without corrosion is recorded in Figure 4A, while the spectrum after immersion into the oil well's formation water without any inhibitor is shown in Figure 5B. Due to the corrosion effect, most of the signals become weaker. In contrast, Figure 4C shows the spectrum of the tubing steel which is immersed into the oil well's formation water with 10 mM (4-chloro-benzylidene)-pyridine-2-yl-amine. Owing to the reduced iron band, a protective film was formed, resulting in a remarkable improvement of the surface state of the tubing steel. Thus, a high level of inhibition efficiency is obtained as the (4-chloro-benzylidene)-pyridine-2-yl-amine attaches firmly to the surface of the tubing steel [30]. This evidence of an inhibition layer formed on the tubing steel surface can explain the inhibition process. In addition, the adsorption isotherm was also studied, to confirm the experiment's results. The surface coverage was utilized to illustrate the adsorption isotherm. The isotherm's parameters and the free energies of the inhibitor's adsorption were calculated and are shown in Table 5.

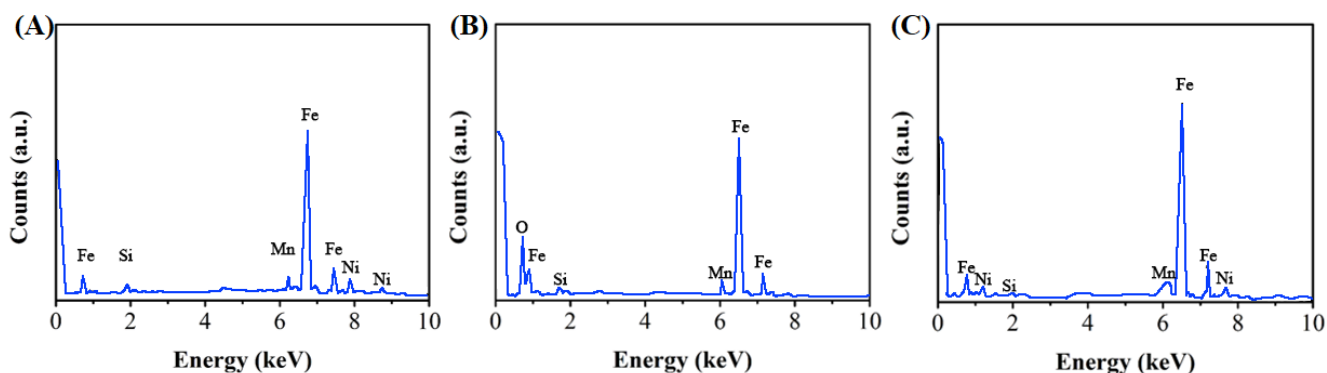


**Figure 4.** EDX of the tubing steel specimens before the immersion into the formation water (A), after the immersion into the formation water (B) in the absence of any inhibitor, and in the presence of (4-chloro-benzylidene)-pyridine-2-yl-amine with a concentration of 10 mM (C).

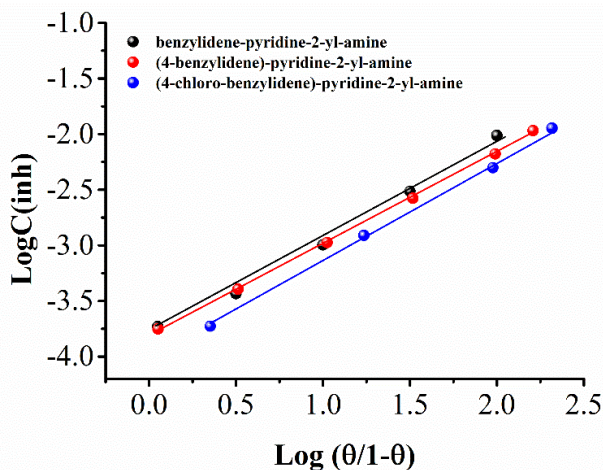


**Figure 5.** Langmuir adsorption isotherm of Schiff bases on the surface of tubing steel.

**Table 5.** The Langmuir isotherm parameters and free energies of adsorption.

Inhibitor	f	B (M)	$\Delta_{\text{ads}}G^\circ$ (M)
Benzylidene-pyridine-2-yl-amine	$5.85 \times 10^{-4}$	$2.63 \times 10^4$	-37.55
(4-benzylidene)-pyridine-2-yl-amine	$6.02 \times 10^{-4}$	$5.37 \times 10^3$	-32.60
(4-chloro-benzylidene)-pyridine-2-yl-amine	$8.61 \times 10^{-4}$	$7.09 \times 10^3$	-31.57

When the adsorption of the inhibitor is assumed to follow the Langmuir adsorption isotherm, the surface coverage can be calculated using the following equation:

$$\theta = \frac{bC_{\text{inh}}}{1 + bC_{\text{inh}}}$$

where the adsorption coefficient is represented by  $b$ . Moreover, using weight loss measurements, the degree of surface coverage ( $\theta$ ) of the inhibitors with various concentrations in acidic media can be assessed using the following equation [29]:

$$\theta = \frac{W - W_{\text{inh}}}{W}$$

where the weight loss of steel with and without inhibitor are expressed as  $W$  and  $W_{\text{inh}}$ , respectively. The values of surface coverage ( $\theta$ ) were graphically tested, to determine whether the data fit a standard adsorption isotherm. A straight line is obtained for the plots of  $\log(\theta/1-\theta)$  as a function of  $\log C_{\text{inh}}$ . This indicates that the adsorption of employed inhibitors on the mild steel surface in a 1 M hydrochloric acid solution obeys the Langmuir adsorption isotherm (Fig. 5).

#### 4. CONCLUSIONS

In conclusion, all Schiff bases studied in this work exhibit outstanding inhibition and could serve as mixed-type inhibitors for the corrosion inhibition of mild steel in the presence of hydrochloric acid. Corrosion inhibition efficiency increased in the following order: benzylidene-pyridine-2-yl-amine, (4-chloro-benzylidene)-pyridine-2-yl-amine, and (4-benzylidene)-pyridine-2-yl-amine. The uniform increase in inhibition efficiency with increased concentration as well as with decrease in  $d\eta/dc$  can be attributed to adsorption phenomenon. The study also found that the adsorption of all additives follows the Langmuir adsorption isotherm. The negative enthalpy values further confirm that this result is due to physical adsorption.

#### References

1. H. Ju, Z. Kai and Y. Li, *Corrosion Science*, 50 (2008) 865.
2. R. Solmaz, E. Altunbaş and G. Kardaş, *Mater. Chem. Phys.*, 125 (2011) 796.
3. A. Asan, S. Soylu, T. Kiyak, F. Yıldırım, S. Öztaş, N. Ancın and M. Kabasakaloğlu, *Corrosion Science*, 48 (2006) 3933.
4. S. Saha, P. Ghosh, A. Hens, N.C. Murmu and P. Banerjee, *Physica. E*, 66 (2015) 332.
5. H. Keleş, M. Keleş, I. Dehri and O. Serindağ, *Colloids and Surfaces A: Physicochemical and Engineering Aspects*, 320 (2008) 138.

6. N. Negm and M. Zaki, *Colloids and Surfaces A: Physicochemical and Engineering Aspects*, 322 (2008) 97.
7. M. Behpour, S. Ghoreishi, A. Gandomi-Niasar, N. Soltani and M. Salavati-Niasari, *Journal of Materials Science*, 44 (2009) 2444.
8. S. Shaban, A. Saied, S. Tawfik, A. Abd-Elaal and I. Aiad, *Journal of Industrial and Engineering Chemistry*, 19 (2013) 2004.
9. W. Mo, H. Xiong, T. Li, X. Guo and G. Li, *J. Mol. Catal. A: Chem.*, 247 (2006) 227.
10. M. Migahed, A. Farag, S. Elsaed, R. Kamal, M. Mostfa and H. El-Bary, *Mater. Chem. Phys.*, 125 (2011) 125.
11. M. Behpour, S. Ghoreishi, M. Salavati-Niasari and N. Mohammadi, *Journal of Nanostructures*, 2 (2012) 317.
12. S. Bilgic and N. Caliskan, *Journal of Applied Electrochemistry*, 31 (2001) 79.
13. S. Hosseini and A. Azimi, *Materials and Corrosion*, 59 (2008) 41.
14. M. Behpour, S. Ghoreishi, M. Salavati-Niasari and B. Ebrahimi, *Mater. Chem. Phys.*, 107 (2008) 153.
15. X. Li, S. Deng, G. Mu, H. Fu and F. Yang, *Corrosion Science*, 50 (2008) 420.
16. U. Naik, V. Panchal, A. Patel and N. Shah, *J. Mater. Environ. Sci.*, 3 (2012) 935.
17. I. Aiad and N. Negm, *Journal of Dispersion Science and Technology*, 30 (2009) 1142.
18. M. El-Sukkary, I. Aiad, A. Deeb, M. El-Awady, H. Ahmed and S. Shaban, *Petroleum Science and Technology*, 28 (2010) 1158.
19. S. Ade, M. Deshpande and D. Kolhatkar, *Journal of Chemical and Pharmaceutical Research*, 4 (2012) 1033.
20. H. Shokry, M. Yuasa, I. Sekine, R. Issa, H. El-Baradie and G. Gomma, *Corrosion Science*, 40 (1998) 2173.
21. K. Emregül and O. Atakol, *Mater. Chem. Phys.*, 82 (2003) 188.
22. M. Hosseini, S. Mertens, M. Ghorbani and M. Arshadi, *Mater. Chem. Phys.*, 78 (2003) 800.
23. S. Bilgiç and N. Caliskan, *Appl. Surf. Sci.*, 152 (1999) 107.
24. K. Emregül, R. Kurtaran and O. Atakol, *Corrosion Science*, 45 (2003) 2803.
25. S. Li, S. Chen, S. Lei, H. Ma, R. Yu and D. Liu, *Corrosion Science*, 41 (1999) 1273.
26. F. Bentiss, M. Traisnel and M. Lagrenée, *Corrosion Science*, 42 (2000) 127.
27. B. El Mehdi, B. Mernari, M. Traisnel, F. Bentiss and M. Lagrenée, *Mater. Chem. Phys.*, 77 (2003) 489.
28. F. Bentiss, M. Lagrenée, M. Traisnel, B. Mernari and H. Elattari, *Journal of heterocyclic chemistry*, 36 (1999) 149.
29. L. Vračar and D. Dražić, *Corrosion Science*, 44 (2002) 1669.
30. M. Amin, *Journal of applied electrochemistry*, 36 (2006) 215.